RSC Advances

PAPER

View Article Online
View Journal | View Issue

Cite this: *RSC Adv.*, 2026, **16**, 4241

Polyoxometalate-ionic liquid functionalized magnetic nanocomposites for solid phase extraction and HPLC determination of sulfonamides in food samples

Zahra Nazar,[ab] Ayed M. Binzowaimil,[c] Sidra Iram,[a] Muhammad Tayyab Ishaq,[d] Muhammad Sajid,[a] Hafiz Muhammad Asif,[a] Mohannad Al-Hmoud[c] and Muhammad Salman Khan *[e]

Veterinary drug residues in animal-derived food products raise critical public health concerns, necessitating efficient extraction and detection methods to ensure food safety. In this study, novel Dawson-type polyoxometalate-ionic liquid (POM-IL) functionalized magnetic nanocomposites were synthesized for magnetic solid-phase extraction (MSPE) followed by high-performance liquid chromatography-ultraviolet (HPLC-UV) detection of sulfonamide residues, sulfamerazine (SMR), sulfamethazine (SMZ), and sulfamethoxazole (SMX) in milk, honey, and egg samples. The POM-ILs were immobilized onto Fe_3O_4@SiO_2 nanoparticles to form MNP@POM-Q^8IL and MNP@POM-Q^{10}IL sorbents, which were characterized by FTIR, PXRD, SEM, and TGA analyses. The Q^{10}-based composite exhibited superior adsorption efficiency, attributed to its longer alkyl chain that enhances hydrophobic interactions and molecular affinity while reducing matrix effects. The synergistic integration of POM, ionic liquid, and magnetic nanoparticle components enhances interfacial molecular recognition and adsorption efficiency, providing a rapid, reusable, and green platform for the sensitive HPLC determination of sulfonamide residues in food matrices. Under optimized conditions, the developed method showed excellent linearity (0.02–1000 μg mL^{-1}), low detection limits (0.03–0.6 μg mL^{-1}), high recoveries (up to 99%), and good reusability over eight extraction cycles. This work provides a rapid, green, and highly efficient analytical platform for the selective extraction and sensitive determination of veterinary drug residues in complex food matrices.

Received 8th November 2025
Accepted 9th December 2025

DOI: 10.1039/d5ra08607h

rsc.li/rsc-advances

1. Introduction

Drug residues are the main food safety concern. Antibiotics are likely to remain in food and seriously threaten people's health.[1–3] Sulfonamides (SAs) are a common class of antibiotics containing a *p*-aminobenzene structure and are widely used in both human and veterinary medicine due to their low cost, high efficiency, and excellent antibacterial properties against common bacterial diseases, making them popular therapeutic agents.[17] They play a vital role in preventing infections and promoting animal health. However, uncontrolled use of these drugs can lead to their accumulation in animal tissues and transfer into their food products, posing a serious public health concern.[45,46] The presence of sulfonamide residues in food products of animal origin has been linked to increased antimicrobial resistance and adverse physiological effects, including potential carcinogenicity, hypersensitivity reactions, severe allergic responses, bone marrow suppression, and urinary system damage. SAs, in particular, sulfamerazine (SMR), sulfamethazine (SMZ), and sulfamethoxazole (SMX) have diverse applications and are commonly detected as simultaneous residues, increasing their potential risk. Regulatory authorities establish maximum residual limits (MRLs) to protect consumer safety. For example, the MRL for all sulfonamides within animal-derived items such as milk, honey and eggs has been set by the European Union at 100 μg L^{-1}.[43]

Growing concern over environmental sulfonamide (SA) residues has highlighted the need for reliable detection methods. However, their low concentrations and complex food matrices present analytical challenges. Thus, developing sensitive, rapid, and cost-effective methods for detecting

[a]*Institute of Chemical Sciences, Bahauddin Zakariya University, Multan, 60800, Punjab, IR Pakistan*
[b]*School of Molecular Sciences, University of Western Australia, Australia*
[c]*Department of Physics, College of Science, Imam Mohammad Ibn Saud Islamic University (IMSIU), Riyadh, 13318, Saudi Arabia*
[d]*Department of Chemistry, University of Southern California, Los Angeles, CA 90089, USA*
[e]*Department of Physics, Abdul Wali Khan University, Mardan, 23200, Pakistan. E-mail: salmankhan73030@gmail.com*

sulfonamide residues in food products remains essential for monitoring residues below maximum residue limits (MRLs).[13,30] Various analytical techniques, including capillary electrophoresis,[52] GC-MS,[41] LC-MS/MS,[55] and HPLC with detectors such as fluorescence,[53] MS,[39,54] and UV,[20] have been employed. UV remains the most commonly used due to its cost-effectiveness, although other detectors offer greater sensitivity at higher operational costs. Despite the sensitivity of chromatographic techniques, trace-level detection is often limited by matrix interference, necessitating effective pretreatment. Reported approaches include DLLME,[47] d-SPE,[23] LLE,[50] SPE,[36] and MSPE.[38] Among these, MSPE stands out due to its simplicity, high enrichment factor, short extraction time, low solvent consumption, minimal instrumentation, and compatibility with both online and offline analytical systems.[31] The use of magnetic nanoparticles (MNP) enables efficient pollutant adsorption from aqueous samples with minimal material input, making MSPE a widely adopted technique for trace analysis in food and environmental samples. The extraction efficiency of target analytes depends on the efficiency of the adsorptive material. Various materials have been utilized to extract sulfonamides. These materials have included polypyrrole,[48,49] covalent organic frameworks,[22] metal–organic frameworks,[32,33] carbon nanotubes,[56,57] magnetic mesoporous carbon,[29] molybdenum-based nanocomposites,[55] graphitic materials,[24] magnetic molecularly imprinted polymer,[10,11] and poly (ethylene glycol) diacrylate.[36]

An interesting material for extracting sulfonamides from complex materials is polyoxometalate-ionic liquids (POM-ILs). Polyoxometalates (POMs) are inorganic metal-oxo nanoclusters with the general formula $[X_xM_mO_o]^{n-}$, where X is a heteroatom, and M is an early transition metal (TM) ion at its highest oxidation state (W^{6+}, Mo^{6+}, V^{5+}) (Dawson 1953). Under certain circumstances, an early transition metal cation and oxygen atoms condense to form POMs, which are usually oxyanions. The general formula of Dawson polyoxometalate (WD POM), a common POM type, is $[X_2M_{18}O_{62}]^{n-}$, where M serves as an early transition metal ion or additional atom (molybdenum, tungsten) and X is a heteroatom (phosphorus, silicon, sulfur, arsenic, *etc.*).[34] In 1953, the very first Dawson POM was designed and published.[19] Salts that consist of large organic cations and small organic or inorganic anions are known as ionic liquids (ILs). Sorbents that incorporate immobilized or impregnated ionic liquids with various support materials have been increasingly popular in extraction procedures for enrichment purposes in recent years.[51] Particularly, nanomaterials have been exploited for organic compound adsorption thanks to their larger specific surface areas, which can enhance adsorption capabilities.[3–5] The material properties are significantly enhanced by the synergistic interactions that are generated by the incorporation of ionic liquids with solid support materials (Fe_3O_4@SiO_2). ILs are highly effective for extraction methodologies due to their ability to establish multiple intermolecular interactions, including hydrophobic, electrostatic, and π–π interactions with a variety of analytes, which is a result of their unique chemical architectures.[6] Moreover, the enhanced thermal and mechanical robustness of ionic liquids has substantially expanded their applications in modern extraction processes. In the area related to analytical chemistry, the preparation of more novel sorbents with strong extraction capabilities remains a challenging task.

In this work, we developed Dawson-type polyoxometalate-ionic-liquid (POM-IL) hybrids immobilized onto Fe_3O_4@SiO_2 magnetic nanoparticles to synthesize multifunctional sorbents with tunable surface chemistry, high adsorption capacity, and magnetic recoverability. Two composites, MNP@POM-Q^8IL and MNP@POM-Q^{10}IL, were synthesized using quaternary ammonium cations with different alkyl chain lengths to assess the effect of hydrophobicity on extraction efficiency. The longer alkyl chain of the Q^{10} cation enhances hydrophobic interactions and molecular affinity, improving adsorption selectivity toward sulfonamide antibiotics. The synthesized sorbents demonstrated efficient and environmentally friendly magnetic solid-phase extraction (MSPE) performance, followed by the HPLC-UV detection for the determination of sulfonamide residues in milk, honey, and egg samples. The developed composites offer high sensitivity, superior extraction efficiency, operational simplicity, and reusability, establishing POM-IL-based magnetic nanocomposites as promising sorbents for food safety monitoring.

2. Materials and methods

2.1. Materials and reagents

Every reagent used had the highest level of purity and was of the best analytical standard. The following items were bought with 98% purity: ferrous sulfate ($FeSO_4 \cdot 7H_2O$), sodium tungstate (Na_2WO_4), sodium metasilicate (Na_2SiO_3), ammonium chloride (NH_4Cl), potassium chloride (KCl), ferric chloride hexahydrate ($FeCl_3 \cdot 6H_2O$), tetra-octyl ammonium bromide $[CH_3(CH_2)_7]_4$-N(Br), and tetrakis(decyl) ammonium bromide $[CH_3(CH_2)_9]_4$-N(Br) as well. Sigma-Aldrich, Germany, supplied analytic-grade criteria for pharmaceuticals, such as sulfamerazine (SMR, 98%), sulfamethazine (SMZ, 98%), and sulfamethoxazole (SMX, 99%). The well-established research methodology approach was used to synthesize Well-Dawson POM, as shown in the supplementary data.[12]

2.2. Instruments and conditions

The prepared materials were analyzed using multiple characterization techniques. In this study, Fourier transform infrared spectroscopy (FTIR) was employed to identify the functional groups present in the produced composites. A Shimadzu FTIR-8400S was used to record the FT-IR spectra at room temperature, comprising the wavenumber range of 4000 to 500 cm^{-1}. Using the SDT Q600 V20.9 Build 20, thermogravimetric analysis (TGA) was performed over a temperature range of 20 °C to 600 °C at a heating rate of 5 °C min^{-1} and a nitrogen flow rate of 100 mL min^{-1}. Utilizing powdered X-ray diffraction (PXRD, Powder D8 Advance, Bruker Germany) throughout a 2θ range of 10–70°, the crystalline structure and phase composition of the synthesized composite were examined. The magnetic properties of the developed composite were investigated with a VSM (Model

7407, Lakeshore, USA). A scanning electron microscope (SEM) was used to examine the surface topography. Quantification of drug residues was done by means of a high-performance liquid chromatography (HPLC) system (Shimadzu 10A). A Welchrom ®C18 column (4.6250 mm, 5 μm Waters-Alliance, USA), a UV-VIS detector SPD 10A, and two pumps (LC 10AT, CBM-102, and CTO 10A) were operated to perform the chromatographic separations. The complete duration of the run was 15 minutes, with a 1 mL min^{-1} flow rate. For inserting the sample, it was connected to the manual valve for injection by a sampling loop of 20 μL. The isocratic elution with the mobile phase was methanol and water (30 : 70) (v/v) ratio. The prepared mobile phase was filtered using a 0.22 μm nylon filter. All the drug samples were filtered through a syringe filter before chromatographic analysis.

2.3. Synthesis of POM-IL

The POM-IL was synthesized by mixing two separate solutions. The first solution was prepared by dissolving 0.60 g of Dawson-type heteropoly acid ($H_6P_2W_{18}O_{62}\cdot 14H_2O$) in 50 mL of deionized water and heating it at 50 °C in a round-bottom flask. The second solution was prepared by dissolving 0.55 g of tetraoctylammonium bromide (Q^8Br, 1.18 mmol) in 20 mL of toluene. The two solutions were combined and vigorously stirred for 24 hours at room temperature. The organic phase containing the ionic liquid was separated using a separating funnel, and both toluene and water were removed under reduced pressure. The resulting product was a pale-yellow, highly viscous ionic liquid, which was further purified by solvent stripping three times with chloroform and once with toluene. The molar ratio of $Q^8Br : H_6P_2W_{18}O_{62}$ was approximately 11.5 : 1, corresponding to the exchange of six protons by six tetraoctylammonium cations, forming the ionic liquid salt $(Q^8)_6[P_2W_{18}O_{62}]$.

2.3.1. Synthesis of Fe_3O_4@SiO_2. Fe_3O_4 nanoparticles were synthesized *via* the coprecipitation method as documented in the literature.[51] Deionized water, anhydrous ethanol, and ammonium hydroxide (in a ratio of 10 : 30 : 1 mL) were subsequently combined with 1 g of Fe_3O_4 nanoparticles. This formulation was subjected to ultrasonic treatment for approximately 30 minutes. Following this, 5 mL of tetraethyl orthosilicate (TEOS) was added, and the mixture was stirred for about 22 hours. The resulting Fe_3O_4@SiO_2 composite was then air-dried.

2.3.2. Synthesis of MNP@POM-ILs. To synthesize POM ionic liquids, separate solutions were prepared *via* dissolution of 0.5 g of $(Q^8)_6[P_2W_{18}O_{62}]$ and $(Q^{10})_6[P_2W_{18}O_{62}]$ in acetone (15 mL). 0.5 g of Fe_3O_4@SiO_2 was added to each solution and gently agitated for approximately 24 hours. The acetone was then eliminated under low pressure, and this process was carried out 3–5 times. Following drying by vacuum, the two pure MNP@POM-Q^8IL and MNP@POM-Q^{10}IL products were obtained as dense, easily flowing brownish powders. Based on the reagent ratio and final gravimetric yield, the amount of POM-IL salt supported on Fe_3O_4@SiO_2 was approximately 50 wt%, indicating efficient immobilization of the ionic liquid phase on the magnetic nanoparticles. The composite's synthesis scheme is shown in Fig. 1(A).

2.4. Sample preparation

The stock solutions of individual SAs (SMR, SMZ, and SMX) were prepared by combining 50 mg of each SA with 100 mL of methanol. The solutions were subsequently stored at 4 °C for future use. Equal volumes of each SA solution were combined to prepare these drug solutions. After that, working solutions with different concentrations were made for the analysis by HPLC. Honey, egg, and milk samples were purchased from a local supermarket in Multan, Pakistan. The honey sample was diluted with distilled water in a 2 : 10 (w/w) ratio, filtered through a 0.22 μm syringe filter, and spiked with a known volume of sulfonamide standard solution before solid-phase extraction (SPE). Milk (5 mL) was mixed with 2 mL of acetonitrile (ACN) for deproteinization, centrifuged at 4500 rpm for 10 min, and the resulting supernatant was collected. Egg samples (10 g) were vortexed with 30 mL of ACN for 5 min, ultrasonicated for 30 minutes, followed by a 10-minute centrifugation at 3000 rpm. Sulfonamide stock solutions (100 mg L^{-1}) were prepared in methanol, followed by a mixed standard solution (10 mg L^{-1}) and working solutions in ultrapure water. Spiked samples were obtained by diluting the working solution with the respective sample matrices to the desired concentrations and stored at 4 °C until analysis. For the MSPE process, as shown in Fig. 2(B), a spiked food sample (10 mL) with 15.0 mg of MNP@POM-IL nanocomposite was added, and the mixture was shaken for 10 minutes to facilitate adsorption. The magnetic sorbent was isolated using a neodymium magnet, and the supernatant was discarded. The sorbent was washed with 3.0 mL ultrapure water to remove loosely bound interferents. Desorption was performed by adding 2.0 mL of methanol and shaking for 5 minutes. Finally, the eluent was re-dissolved in 200 μL of mobile phase, after being dried at 60 °C under N_2. After passing through a 0.22 μm syringe filtering system, the extracted eluent was subjected to HPLC-UV analysis.

3. Results and discussion

3.1. Characterization of POM-IL composites

The FT-IR spectra of synthesized POM-Q^8IL, POM-Q10IL, MNP@POM-Q^8IL, and MNP@POM-Q^{10}IL composites are shown in Fig. 2. The bands observed at 3465 and 3486 cm^{-1} are attributed to the stretching vibrations associated with the tetraoctyl ammonium cations in the Dawson-type POM-IL composite.[7,8] A characteristic peak at 784 cm^{-1}, corresponding to ν(W–O–W) vibrations, confirms the presence of the Wells–Dawson POM in the synthesized ionic liquids and composites.[9] The successful coating of Fe_3O_4 with SiO_2 was confirmed by the presence of Si–O–Si stretching vibrations at 1175, 968, 967, and 963 cm^{-1}. Additionally, the peaks at 1308 and 1047 cm^{-1} were attributed to Fe–O–Si stretching vibrations, demonstrating that the Fe_3O_4 nanoparticles were encapsulated within multiple layers of silica. The low-intensity peak at 587 cm^{-1} corresponds to Fe–O vibrations, further supporting the presence of the Fe_3O_4

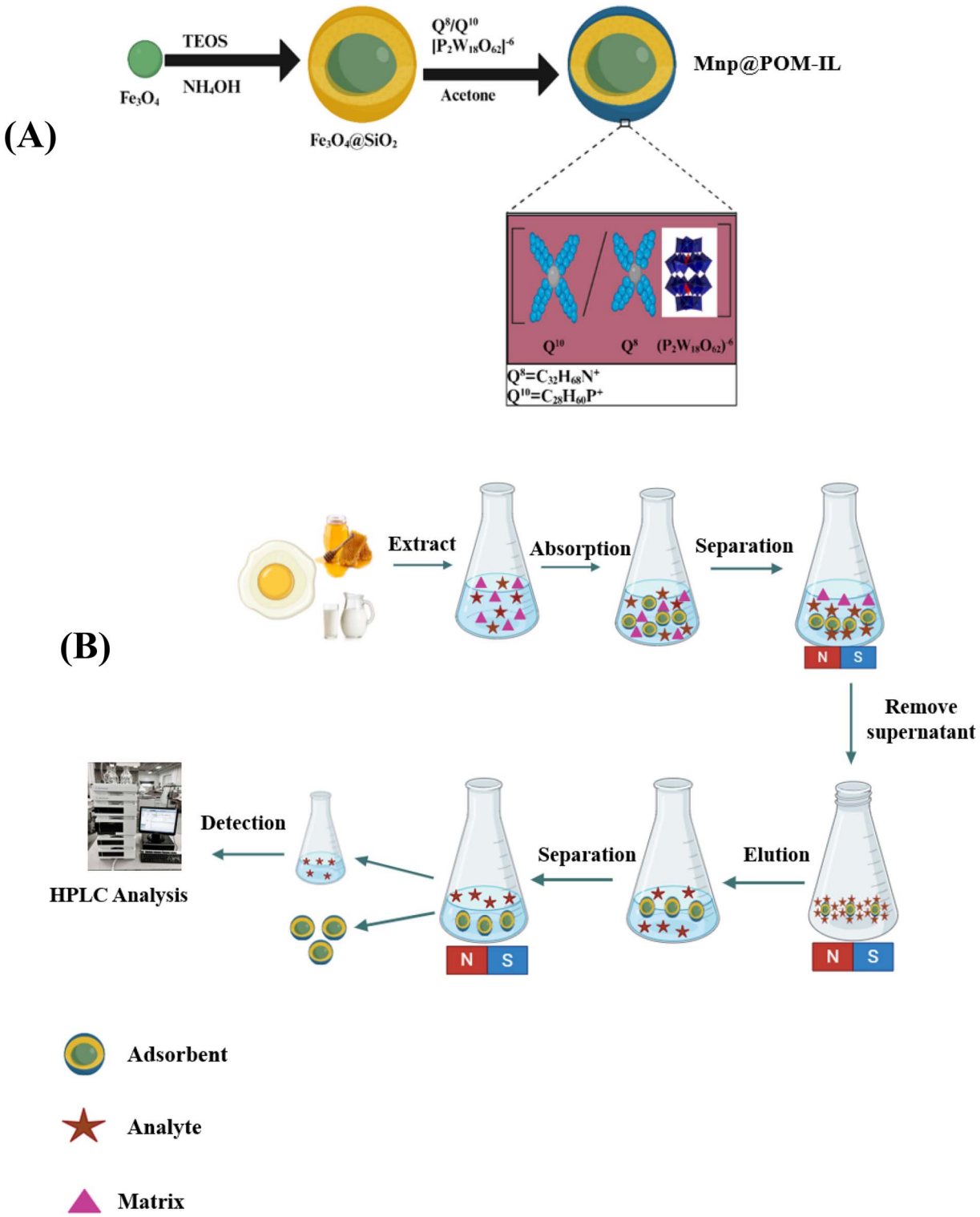

Fig. 1 (A) Schematic of synthesis of MNP@POM-Q^8IL and MNP@POM-Q^{10}IL composites, and (B) process of magnetic solid phase extraction of sulfonamide from food samples.

core. The incorporation of the ionic liquids was confirmed by strong absorption bands at 2959 and 2847 cm^{-1} for MNP@POM-Q^8IL and 2962 and 2843 cm^{-1} for MNP@POM-Q^{10}IL, which correspond to the C–H stretching vibrations of tetraoctyl ammonium (Q^8) and tetrakis(decyl) ammonium bromide (Q^{10}), respectively.[28] These findings confirm the successful functionalization of Fe_3O_4@SiO_2 with Dawson POM-

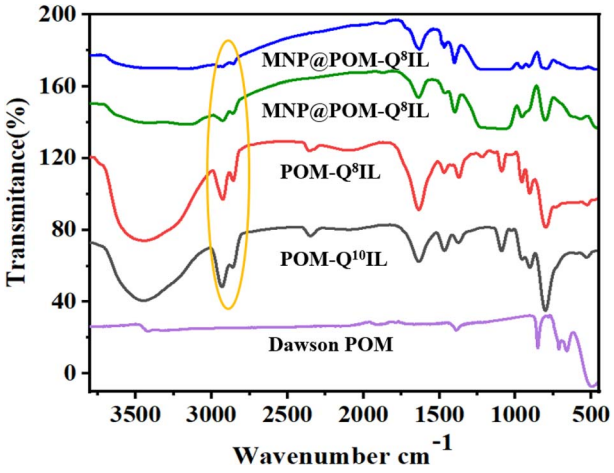

Fig. 2 FT-IR spectra of Dawson POM, POM-Q^8IL, POM-Q^{10}IL, MNP@POM-Q^8IL, and MNP@POM-Q^{10}IL.

IL, forming stable MNP@POM-Q^8IL[2] and MNP@POM-Q^{10}IL composites.

The crystalline nature and structural characteristics of prepared powder samples of POM-Q^8IL, POM-Q^{10}IL, MNP@POM-Q^8IL, and MNP@POM-Q^{10}IL were examined using PXRD. The samples of the prepared composites were analyzed on PXRD using Cu Kα radiation at a wavelength of Å. The suggested pattern (Fig. 3) demonstrates the presence of Fe_3O_4, SiO_2, and Dawson POM-IL distribution in the PXRD pattern of the prepared composites. The adsorbent's good crystalline nature was evident from the display of a variety of diffraction signals in the 20° to 70° range at 2θ. The PXRD peaks at 23.72°, 25.17°, 28.54°, 38.64°, 42.01°, 44.42°, 47.20°, 53.45°, 55.48°, and 56.35° match well with the standard diffraction pattern of tungsten oxide (JCPDS card no. 43-1035).[37] The XRD pattern confirms the structure of Fe_3O_4, indexed to (JCPDS card no. 03-0863), with peaks at $2\theta = 30.27°$, 32.10°, 43.42°, 53.48°, 56.35°, and 63.02°.[25] The sharp peak from $2\theta = 27°$ is consistent with the silica phase

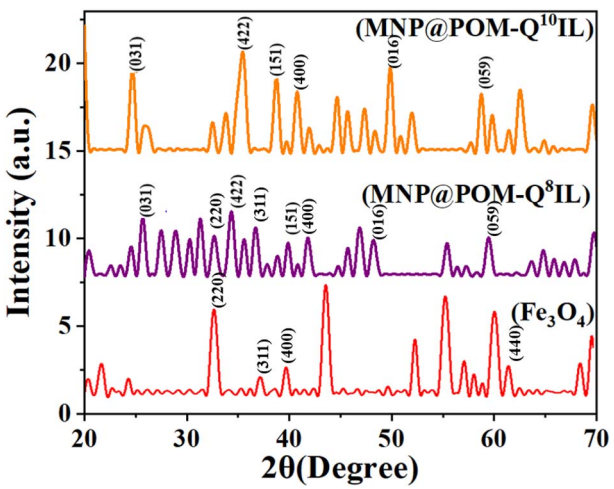

Fig. 3 XRD of Fe_3O_4, MNP@POM-Q^8IL, and MNP@POM-Q^{10}IL showing the different diffraction peaks at 2θ in the range of 10° to 70°.

in the shell of the silica-coated Fe_3O_4 nanoparticles (Fe_3O_4@-SiO_2).[18] Consequently, the strong diffraction showed that the synthesized MNP@POM-IL composites had a crystalline assembly. All additional peaks in the diffraction pattern indicate the presence of organic content.

To determine the thermal stability of synthesized ionic liquid composites MNP@POM-Q^8IL and MNP@POM-Q^{10}IL, thermogravimetric analysis was performed using a heating range of 50 to 600 °C in a nitrogen atmosphere. The TGA curves for MNP@POM-Q^8IL and MNP@POM-Q^{10}IL are shown in green and blue lines, respectively, in Fig. S1. At temperatures between 300–550 °C, weight loss is minimal and maximum at 200–300 °C.[42] Typically, thermal analysis has demonstrated the water loss of POM within the 300-degree Celsius range,[1] and this produced POM anion demonstrated the degradation between 350 and 550 °C.[35] Tungsten metal is thermally stable under relatively lower temperatures because of its elevated melting temperature (3422 °C).[14] The inorganic POM anionic compounds, as well as these cations, at temperatures from 300 to 500 °C (Q^8, Q^{10}), exhibited a curved line of decomposition. Three steps were taken to complete decomposition. The initial mass reduction observed between 20 °C and 200 °C was attributed to the evaporation of water, residual ethanol/methanol, and toluene solvent. The ensuing weight loss, which happened around 200 to 400 degrees Celsius, was linked to MNP@POM-ILs' alkyl chain's thermal degradation. The breakdown of the tungsten of MNP@POM-IL was responsible for the weight decrease during the third phase.

The TGA curve indicated that MNP@POM-Q^{10}IL maintains outstanding thermodynamic stability at elevated temperatures. Analysis of TGA further confirmed higher thermal resistance and minimal mass loss of the MNP@POM-IL composites.[27] The morphology and microstructure of synthesized MNP@POM-Q^8IL and MNP@POM-Q^{10}IL composites were characterized by SEM, as shown in Fig. S2. The SEM image of MNP@POM-Q^8IL (Fig. S2a) shows a densely packed, rough surface comprising aggregated nanoparticles, confirming effective surface modification with the POM-based ionic liquid.[3] In comparison, MNP@POM-Q^{10}IL (Fig. S2b) presents a similarly rough morphology but with more dispersed particles, likely due to the longer alkyl chains of the Q^{10} cations reducing interparticle aggregation. The irregular, interconnected structures observed in both composites indicate successful IL functionalization and provide a high surface area conducive to efficient analyte interaction during magnetic solid-phase extraction (MSPE). The magnetic properties of Fe_3O_4, MNP@POM-Q^8IL, and MNP@POM-Q^{10}IL were assessed by VSM (Fig. S3). Fe_3O_4 showed a high saturation magnetization (Ms) of 75 emu g^{-1}, indicating strong magnetic behavior. Surface modification with non-magnetic POM-ILs reduced the Ms to 38 emu g^{-1} for MNP@POM-Q^8IL and 35 emu g^{-1} for MNP@POM-Q^{10}IL, due to increased composite mass and dilution of magnetic content. Despite this reduction, both composites retained sufficient magnetization for rapid magnetic separation. The lack of coercivity and remanence confirms superparamagnetic behavior, which is suitable for preventing aggregation and

enabling reuse in MSPE, thereby confirming their suitability for sulfonamide extraction from food samples.

3.2. Optimization conditions of HPLC

A number of critical factors for the MSPE method, such as the adsorbent amount, pH of the sample, time, eluting solvent, eluent volume, as well as reusability cycles, were adjusted in order to achieve the optimum extraction efficiency for SAs. The efficiency of the extraction method is strongly affected by the amount of adsorbent used. To evaluate this parameter, experiments were carried out with adsorbent doses ranging from 5 to 25 mg. Increasing the dosage from 5 to 15 mg resulted in a noticeable improvement in extraction efficiency, which can be attributed to the increased surface area and the greater number of active sites available for sulfonamide adsorption. However, beyond 15 mg, no significant enhancement in extraction efficiency was observed (Fig. 4(i)). Consequently, 15 mg in 10 mL of sample solution was selected as the optimal adsorbent dosage for subsequent experiments, balancing high extraction performance with minimal material consumption. The targeted SAs' charge distributions are impacted by the pH of the sample solution, which in turn affects the analyte–adsorbent interaction and extraction efficiency. pH of the experimental solution was systematically evaluated in the specified range of 2 to 10 to ensure accurate and reliable results. As the pH increases from 2 to 6, analyte extraction efficacy improves, but it decreases beyond pH 6, emphasizing the need for optimal pH levels in extraction processes. The extraction efficiency of sulfonamides (SAs) was maximized at a pH of 6 since these compounds and sorbent materials do not interact hydrophobically. Consequently, analytes were extracted simultaneously at a pH of 6. As shown in Fig. 5(ii), the data demonstrate that extraction efficiencies did not increase under alkaline conditions. Unlike alkaline environments, acidic conditions facilitate the protonation of nitrogen atoms in the sulfonamide structure, significantly improving desorption from the adsorbent surface. The effectiveness of the method and the extraction efficiency of analytes are significantly affected by both the type and the volume of eluent utilized. Selecting the right eluent and adjusting its volume are critical factors that directly determine the success of the extraction process and the quality of the results obtained. Therefore, choosing the appropriate eluent and its volume is crucial for optimizing performance and achieving the best analytical results.

The analytes are efficiently desorbed or eluted by a suitable solvent from the adsorbent. First, the impact of methanol, acetonitrile, isopropanol, and ACN on elution was examined to accomplish this objective, as illustrated in Fig. 4(iii). The extraction efficiency was highest in methanol. Consequently, we determined that methanol would be the eluting solvent for subsequent procedures. This variation in extraction efficiency with solvent type arises from differences in interactions at the active sites of MNP@POM-IL. Oxygen-rich POM sites enable hydrogen bonding, while IL cations provide hydrophobic domains. Polar solvents compete with analytes for hydrogen bonding, reducing adsorption, whereas less polar solvents

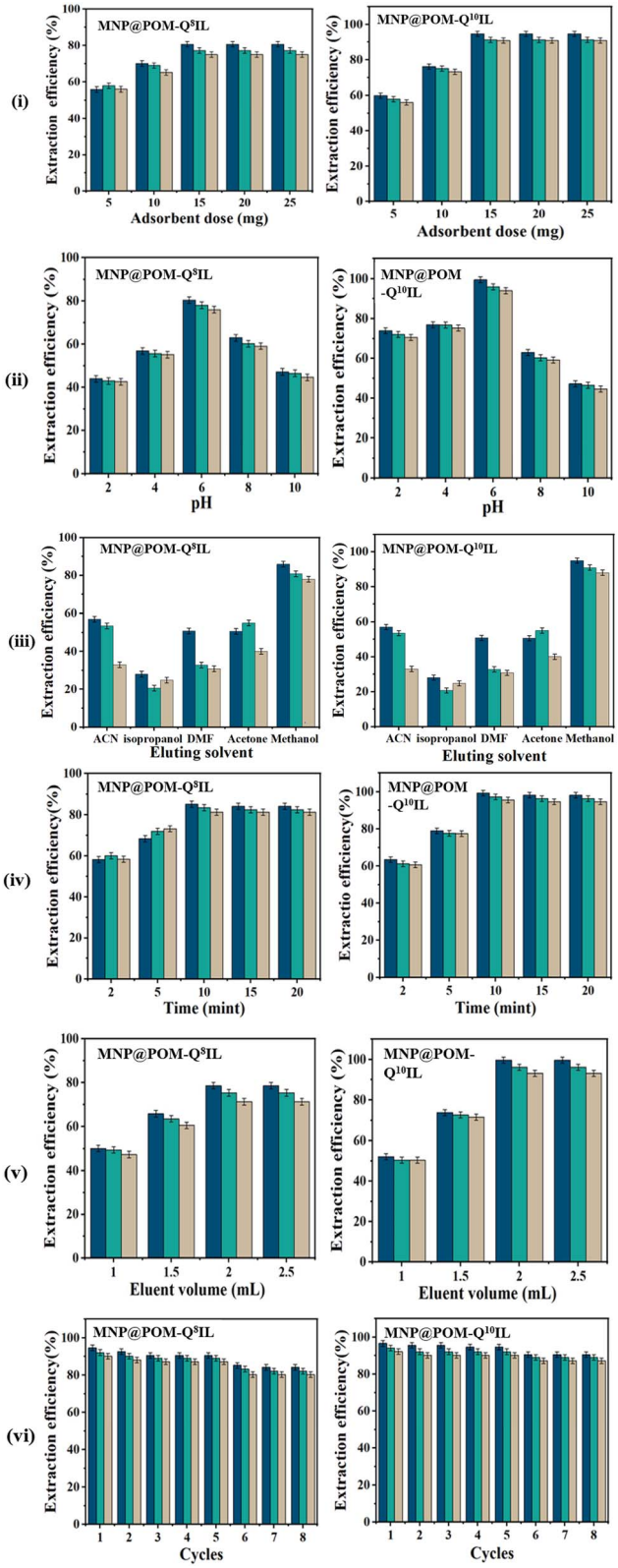

Fig. 4 Optimization of HPLC conditions (i) adsorbent dose, (ii) pH, (iii) eluting solvent, (iv) eluent volume, (v) time, (vi) reusability. SMR SMZ SMX.

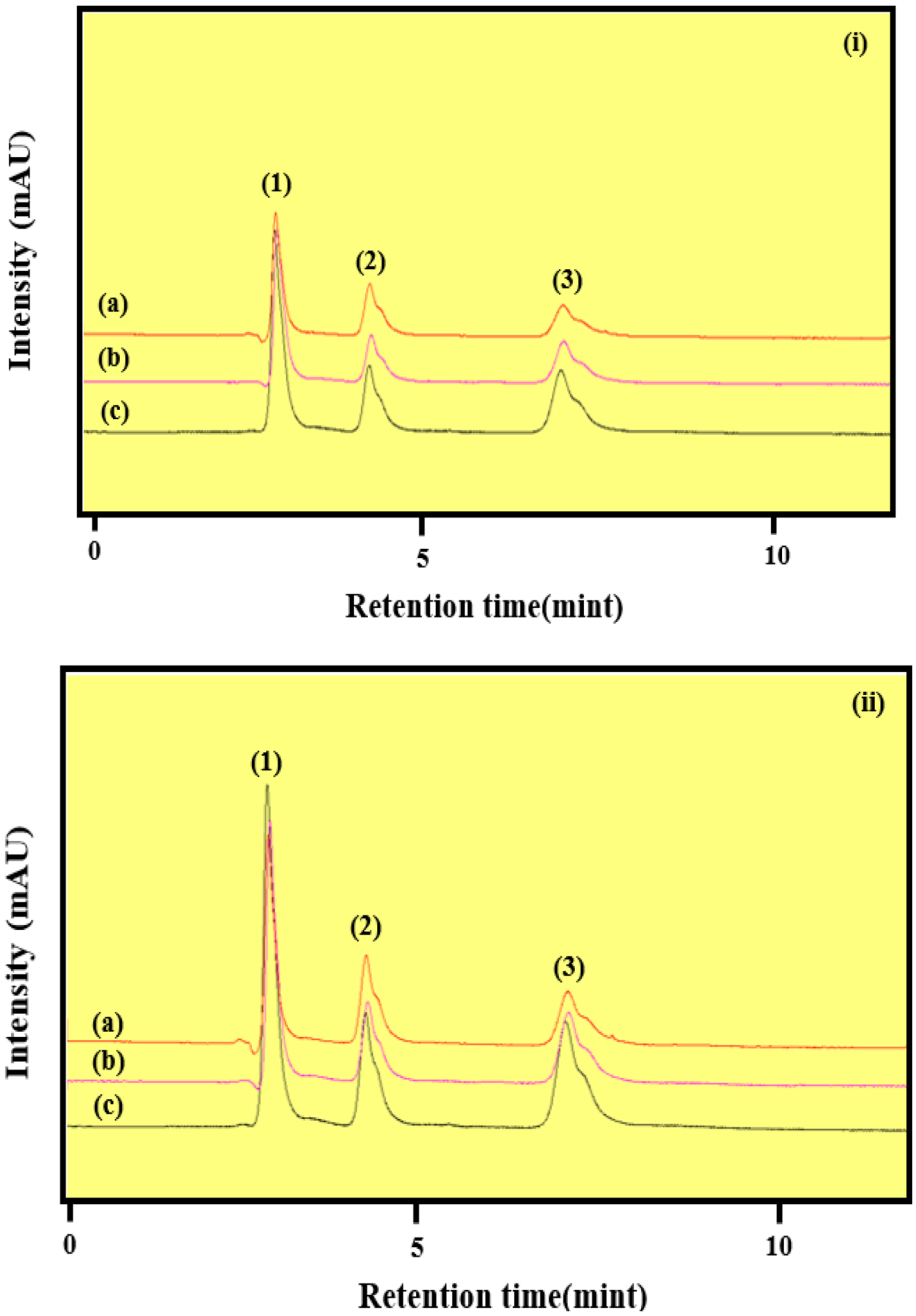

Fig. 5 HPLC chromatograms of sulfonamide residues extracted from (a) honey, (b) milk, and (c) egg samples using (i) MNP@POM-Q^{8}IL and (ii) MNP@POM-Q^{10}IL sorbents. Peak 1 → sulfamerazine (SMR); Peak 2 → sulfamethazine (SMZ); Peak 3 → sulfamethoxazole (SMX).

enhance analyte–sorbent interactions. Thus, adsorption efficiency depends on the balance between hydrophilic and hydrophobic sites on the composite surface. The eluting solvent's volume directly influences the analytes' maximum elution from the adsorbent. The amount of methanol was adjusted between 1 and 2.5 mL to maximize this. As seen in the Fig. 5(iv), the findings demonstrated that raising the methanol concentration from 1 mL to 2.5 mL improved the efficiency of extraction. The extraction efficiency is unaffected by further addition of the methanol content. As a result, 2 mL has been selected to be a suitable amount for further research.

Optimizing extraction efficiency in any process requires striking a balance between the analyte drug solution along the extraction procedure. Maintaining this balance is crucial for optimizing efficacy and achieving the intended outcomes. To assess the impact of various time intervals on the adsorbent and target analytes, the duration of extraction was varied from 2 to 20 minutes. The extraction efficacy of the analytes improves with greater contact time, as demonstrated in Fig. 5(v). The extraction efficiency remained unaffected after 10 minutes, suggesting that the maximum extraction was achieved. To evaluate the practical applicability and economic feasibility of

the synthesized magnetic sorbent, its reusability was systematically investigated. Following each extraction cycle, the sorbent was regenerated through sonication in a 5 mL water–ethanol mixture for 10 minutes, then thoroughly washed and dried. The regenerated sorbent was subsequently employed under optimized MSPE conditions over eight consecutive cycles as shown in Fig. 5(vi). The extraction efficiency remained consistently high across all cycles, demonstrating the composite's excellent chemical stability, low activity loss, and strong potential for repeated analytical use.

3.3. Interaction mechanism

The extraction of sulfonamides using Dawson POM-based ionic liquid-functionalized Fe_3O_4@SiO_2 composites is governed by a synergistic mechanism involving multiple interactions. Strong electrostatic attraction occurs between the anionic Dawson POM clusters and the protonated amine groups of sulfonamides, while hydrogen bonding is facilitated by POM and silanol oxygen atoms with the $-SO_2NH_2$ groups. Simultaneously, the long hydrophobic chains of Q^{8+}/Q^{10+} cations promote van der Waals and hydrophobic interactions with the aromatic rings of sulfonamides. This cooperative binding network enhances selectivity, adsorption efficiency, and enables rapid and excellent separation.

3.4. Analytical performance

The analytical performance of the composite was evaluated by determining its linear range, limits of detection (LODs), limits of quantification (LOQs), and relative standard deviations (RSDs) using in-column SPE and HPLC-UV under optimal conditions. The linear range for SMR, SMZ, and SMX was 0.2–1000 μg mL^{-1}. The LOD (S/N = 3) ranged from 0.03 to 0.6 μg mL^{-1}, while the LOQ (S/N = 10) was between 0.12 and 1.81 μg mL^{-1} for SMR, SMZ, and SMX. Table 1 presents these results. The method demonstrated high recovery rates of up to 99%, as supported by statistical analysis values for R^2 and the percent relative standard deviation (RSD: 1.02–3.47%) shown in Table 2. The method's precision was evaluated by analyzing the reproducibility (intra-day precision) and the sulfonamide solutions' intermediary reliability (inter-day precision). To enhance the credibility of the proposed method, we meticulously examined its effectiveness under optimized conditions by applying it to various real food samples, such as honey, milk, and eggs. This investigation aimed to detect the presence of sulfonamides in these diverse materials accurately. The chromatograms are shown in Fig. 5. The MSPE method proved to be precise, accurate, and reproducible for drug extraction from food samples. Sulfonamides were spiked into the samples at concentrations of 5, 10, and 20 μg mL^{-1}. As illustrated in Fig. 5, the extracted sulfonamide residues from honey, milk, and egg samples using MNP@POM-Q^8IL and MNP@POM-Q^{10}IL sorbents appeared as distinct chromatographic peaks, confirming successful separation and detection of target analytes. Peak 1 corresponds to sulfamerazine (SMR), Peak 2 to sulfamethazine (SMZ), and Peak 3 to sulfamethoxazole (SMX). The results demonstrate that both sorbents effectively adsorbed and enabled the simultaneous determination of these sulfonamides in complex food matrices. The relative recoveries, presented in Table 2, ranged from 70% to 99%. Synthesized sorbents demonstrated outstanding selectivity and sensitivity, achieving maximum drug recovery.

As shown in Table 2, the extraction efficiency of the sorbents increases with the alkyl chain length of the ionic liquid cation. The MNP@POM-Q^{10}IL composite exhibited higher extraction performance than MNP@POM-Q^8IL, which can be attributed to the increased hydrophobicity and enhanced van der Waals interactions provided by the longer decyl (C^{10}) chain. The longer

Table 2 Analytical performance of the established method for SAs analysis, representing the Intraday and Interday RSDs

		Spike concentration (μg mL^{-1})			Recovery (%)		
Adsorbent	Food sample	SMR	SMZ	SMX	SMR	SMZ	SMX
MNP@POM-Q^8IL	Milk	5	5	5	78	80	77
		10	10	10	73	73	70
		20	20	20	78	76	80
	Honey	5	5	5	79	80	80
		10	10	10	78	74	77
		20	20	20	76	74	75
	EGG	5	5	5	79	80	7
		10	10	10	72	78	72
		20	20	20	73	74	72
MNP@POM-Q^{10}IL	Milk	5	5	5	95	93	91
		10	10	0	96	94	95
		20	20	20	96	99	92
	Honey	5	5	5	98	94	91
		10	10	0	93	94	91
		20	20	20	94	95	90
	EGG	5	5	5	92	91	92
		10	10	0	93	97	92
		20	20	20	95	94	93

Table 1 Analytical performance of the established method for SAs analysis

Adsorbent	Analyte	R^2	LOD μg mL^{-1}	LOQ μg mL^{-1}	Intraday (spiking μg mL^{-1}) RSD			Interday (spiking μg mL^{-1}) RSD		
MNP@POM-Q^8IL	SMR	0.994	0.4	1.22	2.47	1.50	2.66	3.07	3.47	3.32
	SMZ	0.996	0.6	1.81	2.54	2.05	2.01	2.65	2.24	3.18
	SMX	0.998	0.5	1.61	2.85	1.04	2.21	3.17	3.33	3.43
MNP@POM-Q^{10}IL	SMR	0.996	0.03	0.12	1.92	1.02	2.17	2.30	1.38	2.47
	SMZ	0.998	0.05	0.17	2.36	1.79	1.54	2.65	2.64	2.39
	SMX	0.999	0.06	0.20	2.03	1.04	2.32	2.64	2.72	1.62

Table 3 Comparison of the developed method with other methods[a]

Analysis instrument	Type of sample	Sample preparation	Analyte	Linear range (μg mL^{-1})	LOD μg mL^{-1}	Ref.
HPLC-MS/MS	Milk	Vortex-assisted DLLME	Sulfonamides	5–500	0.5–1.5	44
HPLC-UV	Honey, milk	SPE	SDZ, SMZ, SMX	20–800	0.39–0.47	21
HPLC-MS/MS	Milk, meat, egg	SPE	Sulfonamides	0.10–500	0.10–0.60	15
HPLC	Milk, egg	DSPE	Sulfonamides	3–1000	0.93–1.21	40
UHPLC-PDA	Honey	Micro-solid phase extraction	Sulfonamides	3–70	0.9–3.0	26
HPLC	Milk	DSPE	Sulfonamides	1–500	0.4–2.7	22
HPLC-UV	Honey, milk, egg	MSPE	SMX, SMZ, SMR	0.2–1000	0.03–0.6	This work

[a] Abbreviations: HPLC MS-MS: High-Performance Liquid Chromatography-Tandem Mass Spectrometry, DLLME: dispersive liquid–liquid microextraction. HPLC-DAD: high-performance liquid chromatography diode array detector; M-μ-SPE: magnetic micro-solid phase extraction. MSPE, Dispersive magnetic solid-phase extraction, ultra-high-performance liquid chromatography-photodiode array detector (UHPLC-PDA).

alkyl chain improves the affinity between the ionic liquid layer and the relatively hydrophobic sulfonamide molecules, facilitating stronger adsorption at the sorbent interface. The improved extraction efficiency observed for MNP@POM-Q^{10}IL can be attributed to the more hydrophobic and structured interfacial environment created by the longer alkyl chain. This organized surface facilitates stronger molecular recognition through hydrophobic and hydrogen-bonding interactions, thereby enhancing the retention of sulfonamide molecules on the sorbent during extraction. These effects explain the superior extraction efficiency observed for the Q^{10}-based composite."

3.5. Comparison with other methods

A comparative evaluation between the developed analytical method and previously reported techniques is presented in Table 3. The comparison considers key parameters, including the type of sample, analytical instrument used, sample preparation technique, target analytes, linear range, and detection limits (LOD). The findings highlight that magnetic solid-phase extraction (MSPE), utilizing a POM-based ionic liquid composite as the sorbent, provides a fast, efficient, and reliable approach for extracting sulfonamides from complex food matrices. As illustrated in the table, earlier studies have employed various extraction methods, such as DLLME, SPE, and M-μ-SPE, in conjunction with HPLC-UV or HPLC-MS/MS systems. Although MS/MS-based techniques[15,16,44] offer superior sensitivity with LODs as low as 0.10 μg mL^{-1}, they involve expensive and sophisticated instrumentation. On the other hand, HPLC-UV methods *e.g.*, ref. 21 and 47 are more accessible but tend to yield higher LODs and narrower linear ranges. In contrast, the proposed method in this study, combining MSPE with HPLC-UV, achieved excellent analytical performance with low LODs (0.03–0.6 μg mL^{-1}) and a broad linear range (0.2–1000 μg mL^{-1}), making it a cost-effective and practical choice for routine sulfonamide analysis in food samples such as honey, milk, and eggs.

4. Conclusion

In this study, a reusable Dawson-type polyoxometalate (POM) ionic liquid-functionalized magnetic adsorbent was developed in order to selectively remove sulfonamide contaminants in complex food matrices, including milk, honey, and egg samples. The proposed magnetic solid-phase extraction (MSPE) method, followed by HPLC-UV analysis, demonstrated excellent analytical performance regarding recovery, precision, and reproducibility. Among the two synthesized POM-based ionic liquids incorporating quaternary ammonium cations (Q^8 and Q^{10}), the Q^{10} POM composite exhibited superior extraction efficiency. This enhancement is attributed to the longer alkyl chain of Q^{10}, which improved hydrophobic interactions and increased affinity toward sulfonamides, thereby improving adsorption capacity and reducing matrix interferences. Overall, the developed method offers a cost-effective, environmentally friendly, and high-performance approach for monitoring veterinary drug residues in complex food samples. These findings provide valuable insights into the rational design of next-generation IL-based extraction materials and contribute significantly to the field of food safety and residue analysis.

Author contributions

Zahra Nazar: methodology, data curation, software, formal analysis, writing – original draft review & editing. Ayed M. Binzowaimil: data curation, formal analysis, writing – original draft review & editing. Sidra Iram: software, data curation, formal analysis, writing – original draft review & editing. Muhammad Tayyab Ishaq: data curation, formal analysis, writing – original draft review & editing. Muhammad Sajid: data curation, formal analysis, writing – original draft review & editing. Hafiz Muhammad Asif: data curation, formal analysis, writing – original draft review & editing. Mohannad Al-Hmoud: data curation, formal analysis, writing – original draft review & editing. Muhammad Salman Khan: conceptualization, data curation, formal analysis, writing – original draft review & editing.

Conflicts of interest

The authors have no conflicts interest.

Data availability

Data are available upon request from the corresponding author.

Supplementary information (SI) is available. See DOI: https://doi.org/10.1039/d5ra08607h.

Acknowledgements

This work was supported and funded by the Deanship of Scientific Research at Imam Mohammad Ibn Saud Islamic University (IMSIU) (grant number IMSIU-DDRSP2601).

References

1 S. Abednatanzi, K. Leus, P. G. Derakhshandeh, F. Nahra, K. De Keukeleere, K. Van Hecke, *et al.*, *Catal. Sci. Technol.*, 2017, **7**, 1478–1487.
2 H. Ai, Y. Wang, B. Li and L. Wu, *Eur. J. Inorg. Chem.*, 2014, **2014**, 2766–2772.
3 I. Ali, A. Khan, A. A. Basheer, M. Asim and M. K. Almesfer, *Int. J. Biol. Macromol.*, 2019, **132**, 244–253.
4 I. Ali, A. Khan, A. A. Basheer, M. Asim and M. K. Almesfer, *Photochem. Photobiol.*, 2018, **94**, 935–941.
5 I. Ali, A. Khan, A. A. Basheer, M. Asim and M. K. Almesfer, *ChemistrySelect*, 2019, **4**, 12708–12718.
6 S. S. Alterary and A. AlKhamees, *Green Process. Synth.*, 2021, **10**, 384–391.
7 A. V. Anyushin, S. Vanhaecht and T. N. Parac-Vogt, *Inorg. Chem.*, 2020, **59**, 10146–10152.
8 H. S. Chae, S. D. Kim, S. H. Piao and H. J. Choi, *Colloid Polym. Sci.*, 2016, **294**, 647–655.
9 A. Chaudhary, *Phys. Status Solidi A*, 2022, **219**, 2200524.
10 L. Chen, X. Zhang, L. Sun, Y. Xu, Q. Zeng, H. Wang, *et al.*, *J. Agric. Food Chem.*, 2009, **57**, 10073–10080.
11 Z. Chen, Z. He, X. Luo, F. Wu, S. Tang and J. Zhang, *Food Anal. Methods*, 2020, **13**, 1346–1356.
12 R. Contant, W. G. Klemperer and O. Yaghi, *Inorg. Synth.*, 1990, **27**, 104–111.
13 F. Conzuelo, M. Gamella, S. Campuzano, D. G. Pinacho, A. J. Reviejo, M. P. Marco and J. M. Pingarrón, *Biosens. Bioelectron.*, 2012, **36**, 81–88.
14 O. J. Curnow and R. Senthooran, *Polyhedron*, 2023, **233**, 116318.
15 Y. Dai, N. Wu, L. E. Liu, F. Yu, Y. Wu and N. Jian, *Food Chem.*, 2023, **404**, 134671.
16 B. Dawson, *Acta Crystallogr.*, 1953, **6**, 113–126.
17 S. G. Dmitrienko, E. V. Kochuk, V. V. Apyari, V. V. Tolmacheva and Y. A. Zolotov, *Anal. Chim. Acta*, 2014, **850**, 6–25.
18 G. Feng, D. Hu, L. Yang, Y. Cui, X. A. Cui and H. Li, *Sep. Purif. Technol.*, 2010, **74**, 253–260.
19 F. Galán-Cano, R. Lucena, S. Cárdenas and M. Valcárcel, *Microchem. J.*, 2013, **106**, 311–317.
20 X. Geng, S. Lv, J. Yang, S. Cui and Z. Zhao, *J. Environ. Manage.*, 2021, **280**, 111749.
21 X. Han, X. Zhang, L. Zhong, X. Yu and H. Zhai, *Microchem. J.*, 2022, **177**, 107259.
22 Q. Hao, X. Zhou, X. Liang, X. Lai, X. Yan and K. Hu, *Sep. Purif. Technol.*, 2025, 134735.
23 A. V. Herrera-Herrera, M. Asensio-Ramos, J. Hernández-Borges and M. Á. Rodríguez-Delgado, *Talanta*, 2013, **116**, 695–703.
24 S. Iram, Z. Nazar, M. Sajid, T. W. Chamberlain, M. F. Nawaz, M. M. Ahmed and M. Kashif, *Food Chem.*, 2024, **448**, 139022.
25 A. Jalali, I. J. Bari and A. Salehzadeh, *BioNanoScience*, 2024, **14**(5), 5276–5285.
26 W. Khiaophong, P. Suwannasom, N. Teshima, K. Pakkethati, O. Prasitnok and J. Vichapong, *Talanta*, 2025, 128539.
27 H. K. Kim, S. H. Huh, J. W. Park, J. W. Jeong and G. H. Lee, *Chem. Phys. Lett.*, 2002, **354**, 165–172.
28 A. L. Kubo, L. Kremer, S. Herrmann, S. G. Mitchell, O. M. Bondarenko, A. Kahru and C. Streb, *ChemPlusChem*, 2017, **82**(6), 867–871.
29 F. Li, Z. Xue, Y. Shi, J. Xu, Z. Liu, A. Lu and H. Jiang, *J. Chromatogr., A*, 2025, 466160.
30 J. Li, Y. Cai, Y. Shi, S. Mou and G. Jiang, *J. Chromatogr., A*, 2007, **1139**, 178–184.
31 Z. Li, J. Li, Y. Wang and Y. Wei, *Spectrochim. Acta, Part A*, 2014, **117**, 422–427.
32 X. Liu, Y. Tong and L. Zhang, *Food Chem.*, 2020, **303**, 125369.
33 D. Lu, Z. Zhang, X. Li, H. Zhang and Y. Liu, *Anal. Chim. Acta*, 2020, **1133**, 88–98.
34 E. M. Martinis, G. M. Escandar and M. S. Di Nezio, *TrAC, Trends Anal. Chem.*, 2017, **97**, 333–344.
35 U. B. Mioč, R. Ž. Dimitrijević, M. Davidović, Z. P. Nedić, M. M. Mitrović and P. H. Colomban, *J. Mater. Sci.*, 1994, **29**, 3705–3718.
36 A. Moga, M. Vergara-Barberán, M. J. Lerma-García, J. M. Herrero-Martínez and E. F. Simó-Alfonso, *Microchem. J.*, 2020, **157**, 104931.
37 F. A. Mohamed, E. T. Salim and A. I. Hassan, *Dig. J. Nanomater. Biostruct.*, 2022, **17**(3), 1029–1043.
38 Z. Nazar, S. Iram, M. Sajid, H. M. Asif, H. Ullah, R. A. Alshgari and Z. M. Tahroudi, *Microchem. J.*, 2024, **206**, 111650.
39 C. Nebot, P. Regal, J. M. Miranda, C. Fente and A. Cepeda, *Food Chem.*, 2013, **141**(3), 2294–2299.
40 D. T. Pamık, S. S. Bozkurt and T. Mumcu, *Microchem. J.*, 2023, **191**, 108876.
41 T. Portolés, L. E. Rosales, J. V. Sancho, F. J. Santos and E. Moyano, *J. Chromatogr., A*, 2015, **1413**, 107–116.
42 T. Rajkumar and G. R. Rao, *Mater. Chem. Phys.*, 2008, **112**(3), 853–857.
43 Regulation (E. C.), *Off. J. Eur. Communities*, 1990, **224**, 1.
44 H. Shaaban, A. Mostafa, A. M. Alqarni, R. Alsultan, Z. Aljarrash, W. Al-Zawad, *et al.*, *J. Food Compos. Anal.*, 2023, **117**, 105137.
45 Q. Shen, R. Jin, J. Xue, Y. Lu and Z. Dai, *Food Chem.*, 2016, **194**, 508–515.
46 X. Shi, Y. Meng, J. Liu, A. Sun, D. Li, C. Yao and J. Chen, *J. Chromatogr. B*, 2011, **879**(15–16), 1071–1076.
47 A. Shishov, A. Pochivalov, K. Cherkashina and A. Bulatov, *Microchem. J.*, 2020, **158**, 105274.

48 T. Sukchuay, P. Kanatharana, R. Wannapob, P. Thavarungkul and O. Bunkoed, *J. Sep. Sci.*, 2015, **38**(22), 3921–3927.
49 R. Sun, Y. Fang, Y. Li, J. Wei, T. Jiao, Q. Chen, Z. Guo, X. Chen and X. Chen, *Food Chem.*, 2025, **462**, 141007.
50 B. T. Veach, T. K. Mudalige and P. Rye, *Anal. Chem.*, 2017, **89**(6), 3256–3260.
51 Y. Wei, Z. Zhang, Y. Liu and H. Yang, *Procedia Eng.*, 2012, **27**, 632–637.
52 Y. Wu, J. Zhou, X. Wang, Z. Zhang and S. Gao, *J. Chromatogr. Sci.*, 2019, **57**(10), 950–960.
53 L. Yang, Y. Shi, J. Li and T. Luan, *J. Sep. Sci.*, 2018, **41**(7), 1651–1662.
54 X. Yuan, D. Wu, C. Liu, X. Li, Z. Xiong and L. Zhao, *New J. Chem.*, 2018, **42**(24), 19578–19590.
55 Y. Zhao, R. Wu, H. Yu, J. Li, L. Liu, S. Wang, *et al.*, *J. Chromatogr., A*, 2020, **1610**, 460543.
56 Y. Zheng, Z. Zhang, X. Liu, Q. Li and X. Zhao, *Food Anal. Methods*, 2021, **14**, 641–652.
57 A. Zhu, Y. Zhang, J. Wang, Y. Liu, H. Li and H. He, *Food Chem.*, 2022, **391**, 133277.